



# Integrated analysis of immunocyte infiltration and differential gene expression in tricuspid aortic valve-associated thoracic aortic aneurysms

Xiaoping Fan<sup>1#</sup>, Jihai Peng<sup>2#</sup>, Liming Lei<sup>1#</sup>, Jie He<sup>3</sup>, Jinsong Huang<sup>1</sup>, Dingwen Zheng<sup>4</sup>, Wenliu Xu<sup>5</sup>, Shihao Cai<sup>6</sup>, Jimei Chen<sup>1</sup>

<sup>1</sup>Department of Cardiovascular Surgery, Guangdong Cardiovascular Institute, Guangdong Provincial Key Laboratory of South China Structural Heart Disease, Guangdong Provincial People's Hospital, Guangdong Academy of Medical Sciences, Guangzhou 510080, China; <sup>2</sup>Department of Rehabilitation, Guangdong Provincial People's Hospital, Guangdong Academy of Medical Sciences, Guangzhou 510080, China; <sup>3</sup>Department of Vascular Surgery, The First Affiliated Hospital, Sun Yat-sen University, Guangzhou 510000, China; <sup>4</sup>Department of Cardiovascular Surgery, Sir Run Run Shaw Hospital, Zhejiang University School of Medicine, Hangzhou 310016, China; <sup>5</sup>Department of Cardiothoracic Surgery, Zhujiang Hospital, Southern Medical University, Guangzhou 510515, China; <sup>6</sup>Department of Cardiovascular Surgery, Xiamen Cardiovascular Hospital, Xiamen University, Xiamen 361005, China

**Contributions:** (I) Conception and design: X Fan, J Peng; (II) Administrative support: J Chen; (III) Provision of study materials or patients: L Lei, J He, J Huang; (IV) Collection and assembly of data: D Zheng, W Xu; (V) Data analysis and interpretation: X Fan, S Cai; (VI) Manuscript writing: All authors; (VII) Final approval of manuscript: All authors.

<sup>#</sup>These authors contributed equally to this work.

**Correspondence to:** Jimei Chen, MD, PhD. Department of Cardiovascular Surgery, Guangdong Cardiovascular Institute, Guangdong Provincial Key Laboratory of South China Structural Heart Disease, Guangdong Provincial People's Hospital, Guangdong Academy of Medical Sciences, No. 96 Dongchuan Road, Guangzhou 510080, China. Email: jimei@hotmail.com.

**Background:** Progressive dilatation is responsible for significant mortality and morbidity in patients with thoracic aortic aneurysms (TAAs). Studies have shown that the development and progression of TAAs are closely related to immune regulatory pathways and genes. Therefore, it is important to understand the immune regulatory mechanisms and biomarkers of TAA dilatation.

**Methods:** Systematic bioinformatics analysis was applied, including linear models for microarray data (LIMMA) differential expression analyses, principal component analysis (PCA), immunocyte identification, and genetic function enrichment analysis.

**Results:** Our results showed that both aortic intima-media (AMed) and outer aortic adventitia (AAdv) tissues were closely associated with T cell activation during the process of tricuspid aortic valve (TAV)-associated TAA dilation. Additionally, the degree of infiltration of resting memory CD4<sup>+</sup> T cells was linked to both AAdv and AMed vascular dilation. The core regulators PPTRC, IL1B, CD4, CD3G, and IL2RA were also identified and are closely related to resting memory CD4<sup>+</sup> T cell infiltration in this pathological process.

**Conclusions:** The candidate genes PPTRC, IL1B, CD4, CD3G, and IL2RA were involved in the regulation of resting memory CD4 T cell tissue infiltration, which is closely related to the process of AAdv and AMed vascular dilation in TAV patients.

**Keywords:** Thoracic aortic aneurysms (TAAs); pathway enrichment; immunocyte infiltration; integrated bioinformatic analysis

Submitted Nov 20, 2019. Accepted for publication Feb 07, 2020.

doi: 10.21037/atm.2020.03.05

View this article at: <http://dx.doi.org/10.21037/atm.2020.03.05>

## 1 Introduction

2 Thoracic aortic aneurysms (TAAs) are a class of vascular  
3 diseases with rapid progression and very high mortality and  
4 morbidity. Epidemiological studies have suggested that the  
5 overall incidence of TAAs is greater than 7.6/100,000 and  
6 that TAAs are identified in only 78% of patients before  
7 death (1,2). Even with surgical treatment, 16% of patients  
8 died within 30 days after surgery, and the 1-, 5-, and 10-year  
9 survival rates were 92%, 77%, and 57%, respectively, while  
10 the reoperation rate within 10 years was 7.8% (2,3). With  
11 the development of 3D printing technology and hybrid  
12 surgery, the treatment and prognosis of TAAs have greatly  
13 improved (4). However, the mechanisms of TAA occurrence  
14 and progression are still unclear.

15 In recent years, the vigorous development of high-  
16 throughput sequencing technology has provided a new  
17 opportunity for studying the mechanism of TAAs. Studies  
18 have shown that the development and progression of  
19 TAAs are closely related to immune regulatory pathways  
20 and genes. Kim *et al.* investigated gene expression profile  
21 differences between the thoracic aortas of TAA patients  
22 and normal thoracic aortas in organ transplant patients.  
23 They found that the differentially expressed genes  
24 (DEGs) associated with TAAs were mainly associated  
25 with ion transport, cell signal transduction, and immune  
26 inflammatory responses (5). Tang *et al.* analyzed the  
27 pathological process of vascular remodeling (changes  
28 in the vascular outer diameter) and intima dilation in  
29 ascending aorta specimens from TAAs. They found that  
30 the transmural inflammatory state of the aorta and the  
31 production of interferon-gamma (IFN- $\gamma$ ) in TAAs were  
32 closely related to increases in the outer diameter of the  
33 aneurysm, thickening of the intima, maintenance of the  
34 density of vascular smooth muscle cells, and decreases  
35 in matrix proteins (6). Similarly, Sprague *et al.* believed  
36 that the aneurysm dilation process was closely related to  
37 the inflammatory state of blood vessels. Vascular injury  
38 can stimulate the expression of endothelial cell adhesion  
39 molecules and promote the recruitment of inflammatory  
40 cells, growth factors, and cytokines, thus affecting the  
41 functions of vascular smooth muscle cells and endothelial  
42 cells. In addition, these cytokines can induce the production  
43 or activation of vasodilation mediators, such as nitric oxide,  
44 prostacyclin, endothelial-derived hyperpolarizing factors,  
45 and bradykinin, and vasoconstrictors, such as endothelin and  
46 angiotensin II, thereby regulating the pathological process  
47 of vascular dilation (7). However, aneurysm formation is not  
48 always associated with immune inflammation. By comparing

the vascular tissue differential gene expression profiles and  
50 pathological mechanisms of bicuspid aortic valve (BAV)-  
51 and tricuspid aortic valve (TAV)-associated aortic aneurysm  
52 expansion, Folkersen *et al.* found that immune mediators  
53 were activated only in TAV tissues, whereas BAV tissues  
54 did not exhibit a significant immune process. However, the  
55 specific mechanism has not yet been elucidated (8). Based  
56 on this result, this study aimed to conduct an in-depth  
57 investigation of the pathological molecular mechanism of  
58 TAV-associated vascular dilation by analyzing DEGs from  
59 the whole gene expression profile, immune cell infiltration,  
60 and related enrichment pathways in the dilated and  
61 nondilated aortic intima-media (AMed) and outer aortic  
62 adventitia (AAAdv) of TAV patients. This study will provide a  
63 new diagnostic or therapeutic target for this disease.  
64

## 65 Methods

### 66 Data screening and acquisition

67 We downloaded the GSE26155 dataset from the GEO  
68 (<https://www.ncbi.nlm.nih.gov/geo/>) database for subsequent  
69 analysis (9). These data were acquired from microarray  
70 expression profiling of AAAdv and AMed tissues of TAAs  
71 and were published in the Advanced Study of Aortic  
72 Pathology (ASAP). A total of 83 vascular tissue specimens  
73 were selected, including 46 AMed tissue samples (17 dilated  
74 and 23 nondilated samples and 6 boundaries that needed  
75 to be excluded) and 37 AAAdv tissue samples (12 dilated  
76 and 21 nondilated samples and 4 boundaries that needed  
77 to be excluded) (8). The corresponding microarray platform  
78 was the GPL570 (HG U133\_Plus\_2) Affymetrix Human Genome  
79 U133 Plus 2.0 Array platform (Affymetrix, Santa Clara, CA,  
80 USA). In addition, the clinical information corresponding to  
81 each sample was downloaded for further analysis.  
82  
83  
84  
85

### 86 Data analysis

87 The data processing flow was as follows: (I) detection of  
88 the CEL fluorescence intensity; (II) quality control; (III)  
89 background processing using the robust multiarray average  
90 (RMA) method; (IV) processing of missing probe values  
91 by log<sub>2</sub> transformation and the k-nearest neighbor (kNN)  
92 algorithm; (V) gene annotation using probe names; (VI)  
93 differential expression analysis of expression profiles using  
94 linear models for microarray data (LIMMA) (10); and (VII)  
95 examination of the data structure by principal component  
96 analysis (PCA). Cross-checking was applied to identify  
97 DEGs, and then the Benjamini-Hochberg method was  
98

99 used to adjust the statistical P values of the false discovery  
 100 rate (FDR) to calculate the expression fold change (FC) (a  
 101  $\log_2FC > 1.0$  and a corrected  $P < 0.05$  represented DEGs) (10).  
 102 All of the data were obtained from the GEO database, and a  
 103 research ethics application was not needed for this study.

#### 105 *Gene Ontology (GO) and pathway enrichment analysis of* 106 *gene sets*

108 The GO of the AMed- and AAdv-associated DEGs  
 109 was obtained based on analysis using the clusterProfiler  
 110 algorithm (11). The results for co-DEG-related GO and  
 111 Kyoto Encyclopedia of Genes and Genomes (KEGG)-  
 112 enriched pathways were obtained based on an analysis of the  
 113 MetaScape gene annotation and retrieval platform (<http://metascape.org/gp/index.html>) (12).

#### 116 *Analysis of immune infiltration*

118 CIBERSORT (<https://cibersort.stanford.edu/>) is an immune  
 119 cell subtype infiltration calculation algorithm that was  
 120 developed based on linear support vector regression (13).  
 121 Users can comprehensively estimate the infiltration level of  
 122 each cell subtype from chip expression profile and RNA-seq  
 123 expression data. The parameters applied in this study were  
 124 as follows: (I) gene expression values corrected by the RMA  
 125 algorithm; (II) 1,000 deconvolutions (Perm); and (III)  $P < 0.05$   
 126 for differential subtypes.

#### 128 *Association analysis between core genes and differentially* 129 *infiltrating immune cell subtypes*

131 In addition, by constructing the co-DEG-related KEGG  
 132 pathway network, pathway-rich genes of interest were  
 133 selected for protein-protein interaction (PPI) network  
 134 analysis. The node correlation degree in the network was  
 135 calculated using the STRING database (<https://string-db.org/>) (14) and CytoScape software (15) to identify candidate  
 136 regulatory factors. To further clarify the associations  
 137 between core genes and immune genes, we performed a  
 138 Pearson correlation clustering analysis of candidate genes  
 139 and differential cell subtype infiltration values.

## 142 **Results**

### 144 *Data acquisition and pretreatment*

146 The results of the difference analysis suggested that (I) in the

AAdv tissues, compared with the nondilated group, a total  
 of 1,190 differential mRNAs (3 downregulated and 1,187  
 upregulated) were present in the dilated group; and (II) in  
 the AMed tissues, 173 DEGs were present between the  
 dilated group and nondilated group (7 downregulated and  
 166 upregulated). The distributions of DEGs in AMed and  
 AAdv tissue samples are shown in *Figure 1A* and <http://cdn.amegroups.cn/static/application/d1026d3979cb63f6749fde5efbe1d50d/atm.2020.03.05-1.pdf>.

### *Functional enrichment analysis of DEGs*

In the enrichment analysis, we found that GO:0042110~T  
 cell activation ( $P=1.24E-19$ ,  $n=75$ ), GO:0002694~regulation  
 of leukocyte activation ( $P=1.25E-18$ ,  $n=78$ ), and  
 GO:0001819~positive regulation of cytokine production  
 ( $P=1.38E-16$ ,  $n=70$ ) were closely related to the biological  
 process (BP) of DEGs associated with AAdv dilation,  
 whereas GO:0031012~extracellular matrix ( $P=9.49E-11$ ,  
 $n=60$ ), GO:0009897~external side of the plasma membrane  
 ( $P=2.05E-10$ ,  $n=35$ ), and GO:0062023~collagen-  
 containing extracellular matrix ( $P=3.32E-10$ ,  $n=53$ ) were  
 closely related to the cellular component (CC) of DEGs  
 associated with AAdv dilation. GO:0005201~extracellular  
 matrix structural constituent ( $P=1.60E-10$ ,  $n=32$ ),  
 GO:0005539~glycosaminoglycan binding ( $P=4.68E-05$ ,  
 $n=26$ ), and GO:0008201~heparin binding ( $P=5.88E-04$ ,  
 $n=19$ ) were closely related to the molecular function (MF)  
 of DEGs associated with AAdv dilation (*Figure 1B* and  
<http://cdn.amegroups.cn/static/application/573636b8df0cab7b2c648958a2ea3928/atm.2020.03.05-2.pdf>). Similarly,  
 GO:0042110~T cell activation ( $P=6.61E-17$ ,  $n=27$ ),  
 GO:0001819~positive regulation of cytokine production  
 ( $P=7.35E-15$ ,  $n=25$ ), and GO:0045785~positive regulation  
 of cell adhesion ( $P=3.03E-14$ ,  $n=23$ ) were closely related  
 to the BP of DEGs associated with AMed dilation, while  
 GO:0009897~external side of the plasma membrane  
 ( $P=4.76E-11$ ,  $n=15$ ), GO:0030667~secretory granule  
 membrane ( $P=1.01E-08$ ,  $n=15$ ), and GO:0043235~receptor  
 complex ( $P=7.26E-08$ ,  $n=14$ ) were closely related to the CC  
 of DEGs associated with AMed dilation. GO:0042287~major  
 histocompatibility (MHC) protein binding ( $P=5.78E-07$ ,  
 $n=6$ ), GO:0019955~cytokine binding ( $P=1.55E-06$ ,  $n=8$ ),  
 and GO:0004896~cytokine receptor activity ( $P=4.12E-05$ ,  
 $n=6$ ) were closely related to the MF of DEGs associated  
 with AMed dilation (*Figure 1C* and <http://cdn.amegroups.cn/static/application/573636b8df0cab7b2c648958a2ea3928/atm.2020.03.05-2.pdf>).

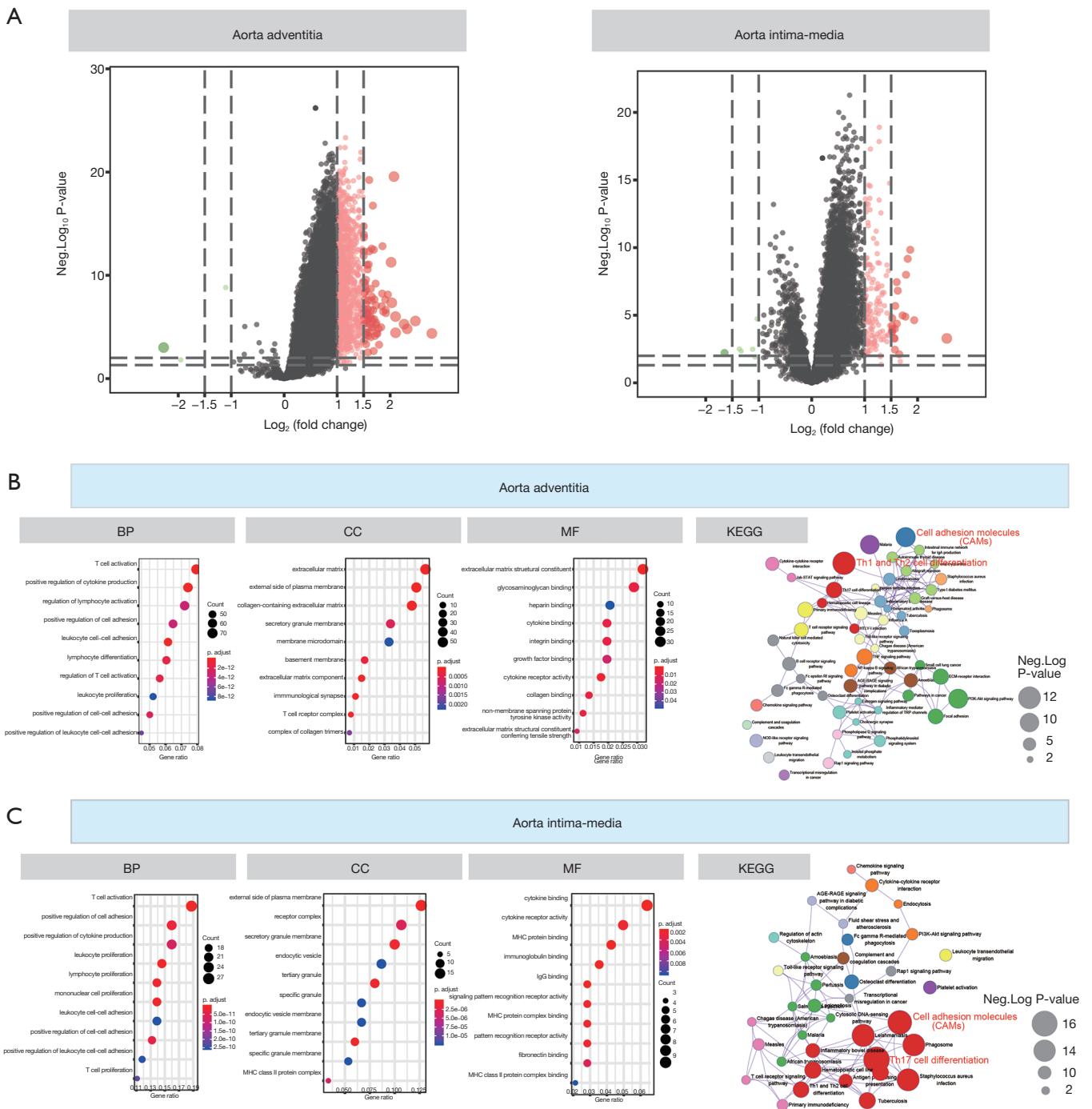


**Figure 1** The differential expression and genetic function enrichment analysis with regard to both aortic intima-media (AMed) and aortic adventitia (AAdv) dilation. The volcano plot in *Figure 1A* presents the differentially expressed genes (DEGs) for the comparison of dilated and nondilated AMed or AAdv samples. *Figure 1B,C* presents the Gene Ontology (GO) and Kyoto Encyclopedia of Genes and Genomes (KEGG) pathway enrichment analyses were performed based on the clusterProfiler and MetaScape databases, respectively. The sizes of the dots represent the counts of enriched DEGs, and the colors of the dots represent the adjusted P value for the GO term enrichment, while the dot size represents the negative Log(P value) for KEGG maps.



195 Analysis of the MetaScape database showed that AAdv-  
 196 associated DEGs were mainly associated with type 1 T  
 197 helper (Th1) and Th2 cell differentiation (enrichment score  
 198 =5.31,  $P=2.51E-11$ ,  $n=25$ ), the PI3K-Akt signaling pathway  
 199 (enrichment score =2.77,  $P=4.00E-10$ ,  $n=46$ ), the tumor  
 200 necrosis factor (TNF) signaling pathway (enrichment score  
 201 =4.0,  $P=4.62E-08$ ,  $n=21$ ), and other pathways (*Figure 1B*  
 202 and <http://cdn.amegroups.cn/static/application/4196621e963294ffbd07d0dc69f03162/atm.2020.03.05-3.pdf>). AMed-  
 203 associated DEGs were mainly associated with Th17 cell  
 204 differentiation (enrichment score =22.50,  $P=1.80E-16$ ,  
 205  $n=15$ ), cell adhesion molecules (CAMs) (enrichment score  
 206 =14.14,  $P=7.23E-15$ ,  $n=17$ ), leishmaniasis (enrichment score  
 207 =23.92,  $P=9.49E-14$ ,  $n=12$ ), and other pathways (*Figure 1C*  
 208 and <http://cdn.amegroups.cn/static/application/4196621e963294ffbd07d0dc69f03162/atm.2020.03.05-3.pdf>).

211

212

### 213 *Identification and functional enrichment of co-expressed* 214 *DEGs in the dilation process of AMed and AAdv tissues*

215 By evaluating the intersection set (*Figure 2*), 107 DEGs  
 216 shared by both AMed and AAdv tissues were obtained  
 217 (*Figure 2A*). PCA showed that co-DEGs could significantly  
 218 distinguish whether AAdv and AMed tissues contained  
 219 dilated blood vessels (*Figure 2C*). Based on cluster analysis,  
 220 the 107 DEGs were divided into five categories. Functional  
 221 enrichment analysis showed that GO:0030334~regulation  
 222 of cell migration, GO:0045785~positive regulation of cell  
 223 adhesion, GO:0002322~B cell proliferation involved in  
 224 the immune response, GO:0045321~leukocyte activation,  
 225 and GO:0002253~activation of the immune response were  
 226 closely related to the functional enrichment of each gene set  
 227 (*Figure 2B* and <http://cdn.amegroups.cn/static/application/bb75016658b7f263c56ab52348e529/atm.2020.03.05-4.pdf>).

229

230

231

### 232 *Core gene identification*

233 Based on the KEGG pathway enrichment network, we  
 234 found that the co-DEGs of AAdv and AMed tissues were  
 235 closely associated with T cell-associated immune pathways  
 236 (*Figure 3A*). We further constructed a PPI network for  
 237 genes enriched in T cell-associated immune pathways and  
 238 found that protein tyrosine phosphatase receptor type C  
 239 (PTPRC) (degree =11), interleukin-1B (IL1B) (degree =7),  
 240 CD4 (degree =7), CD3G (degree =7), and IL-2 receptor  
 241 alpha chain (IL2RA) (degree =11) were closely related to  
 242 the progression of aortic dilation (*Figure 3B*). In addition,  
 compared with the nondilated group, these 5 core genes

were highly expressed in both the AAdv tissues and the  
 AMed tissues in the dilated group (all  $P<0.05$ ; *Figure 3C,D*).

243

244

245

246

247

### *Analysis of immune infiltration*

The overall immune infiltration profiles of AAdv  
 and AMed vascular tissues are shown in *Figure 4A,B*.  
 Resting memory CD4 T cells (AAdv  $P=4.36E-04$ , AMed  
 $P=1.79E-03$ ), regulatory T cells (Tregs) (AAdv  $P=0.027$ ,  
 AMed  $P=1.20E-02$ ), naïve B cells (AAdv  $P=0.044$ , AMed  
 $P=1.90E-02$ ), and monocytes (AAdv  $P=0.051$ , AMed  
 $P=2.10E-02$ ) demonstrated significant differential  
 infiltration in both dilated and nondilated AAdv and  
 AMed tissues (*Figure 4C,D*, <http://cdn.amegroups.cn/static/application/a0d90651ac6c292730150444766be6bb/atm.2020.03.05-5.pdf>).

248

249

250

251

252

253

254

255

256

257

258

Through correlation analysis, we also found that the core  
 regulatory genes (including PTFRC, IL1B, CD4, CD3G,  
 and IL2RA) had strong correlations with the degree of  
 infiltration of resting memory CD4 T cells (AAdv: PTPRC  
 coefficient =0.71, IL1B coefficient =0.52, CD4 coefficient =  
 0.59, CD3G coefficient =0.78, IL2RA coefficient =0.60;  
 AMed: PTPRC coefficient =0.82, IL1B coefficient =0.62,  
 CD4 coefficient =0.78, CD3G coefficient =0.73, IL2RA  
 coefficient =0.64) in AAdv and AMed tissues (*Figure 5A,B*,  
<http://cdn.amegroups.cn/static/application/5c02a2b7023c218db1d6026dae4cf0d1/atm.2020.03.05-6.pdf>).

259

260

261

262

263

264

265

266

267

268

269

270

## 271 **Discussion**

The association between the pathogenesis of TAAs and the  
 immune inflammatory response has always been a popular  
 research topic. Our study found that both AAdv and AMed  
 tissues were closely associated with T cell activation during  
 the process of vascular dilation. By further building a  
 network of disease mechanisms, our results also suggested  
 that PTPRC, IL1B, CD4, CD3G, and IL2RA may be  
 the core regulatory genes of vascular dilation; these genes  
 were closely related to the degree of infiltration of resting  
 memory CD4 T cells in AAdv and AMed vascular tissues,  
 indicating that these genes may be important regulatory  
 mediators in TAA pathogenesis.

271

272

273

274

275

276

277

278

279

280

281

282

283

284

An increasing number of researchers believe that TAAs  
 are immune inflammatory diseases, and the risk of disease  
 increases with increasing age (16). Compared with other  
 aneurysms, the pathological changes in the outer adventitia  
 and media of the aortic wall are more closely associated with  
 the immune inflammatory response, especially those in TAV-

285

286

287

288

289

290

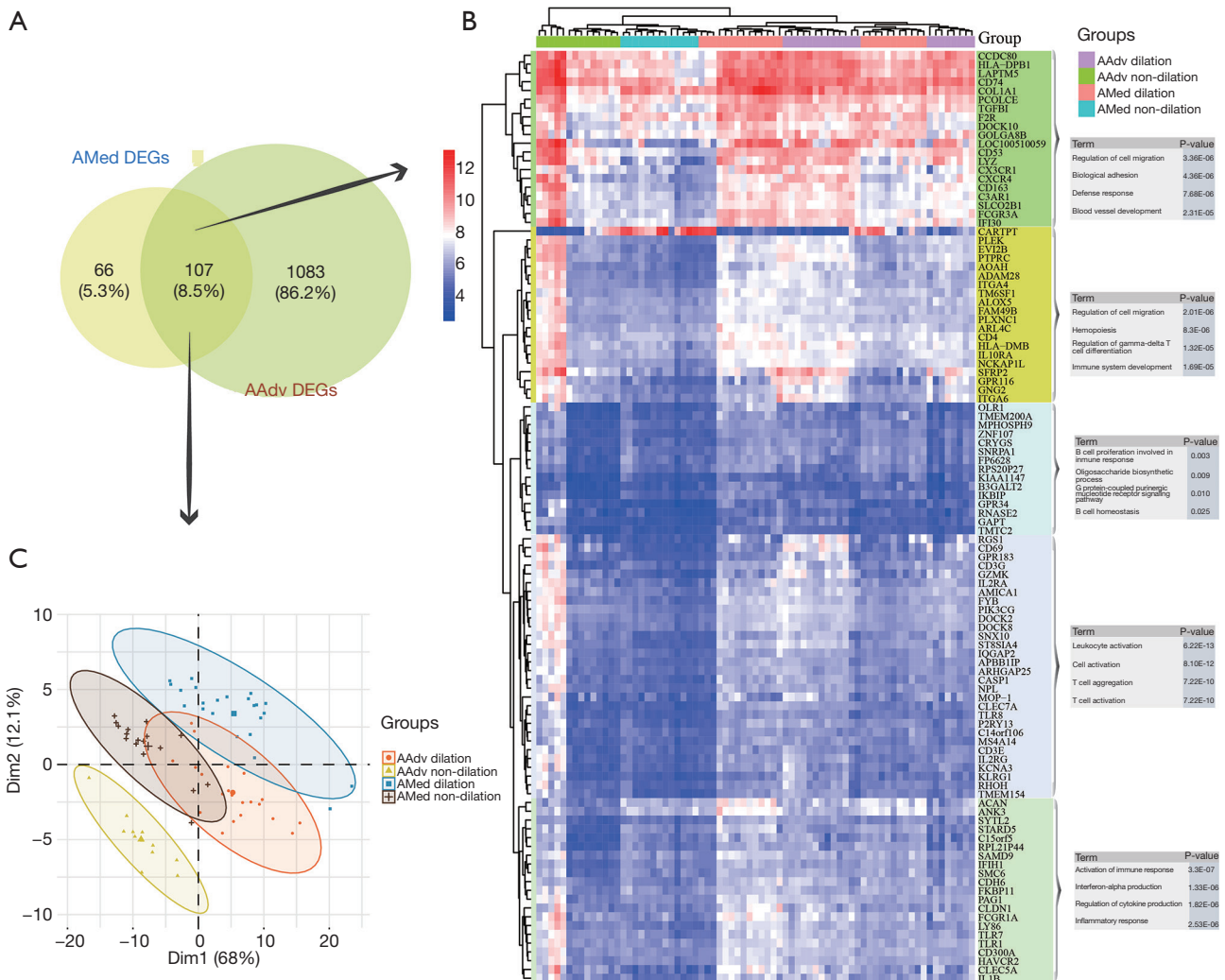


**Figure 2** Co-differentially expressed gene identification and genetic function enrichment analysis. *Figure 2A* indicates the results of overlap for the co-differentially expressed genes (co-DEGs) for the comparison of dilated and nondilated AMed or AAdv samples. The principal component analysis (PCA) in *Figure 2B* shows a significant distribution for the dilated and nondilated AMed or AAdv samples, respectively. *Figure 2C* indicates the results of hierarchical clustering analysis of the co-DEGs for the comparison of dilated and nondilated samples, and the BP terms of the different clusters were also constructed.

291 associated TAA vascular tissues (16,17). Among these changes,  
 292 T cell activation is the most important molecular mechanism.  
 293 Itani *et al.* found that angiotensin II can promote the  
 294 infiltration of leukocytes [CD45 (+)], memory T cells [CD3  
 295 (+)/CD45 Ro (+)] and T lymphocytes (CD3 (+) and CD4  
 296 (+)] in thoracic aortic tissues, increase activated CD4+ and  
 297 CD8+ T cells in the circulation, and increase the production  
 298 of IL17a and IFN- $\gamma$ , suggesting that functional activation  
 299 of T cells and their subpopulations is associated with  
 300 hypertension-induced vascular remodeling and dilation (18).

Similarly, Ju *et al.* found that the cytokine IL6 can induce  
 Th17 lymphocytes to aggregate in dilated vascular tissues  
 through the transcription-3 signaling pathway in an  
 angiotensin II perfusion-induced vascular dissection model.  
 At the same time, these lymphocytes promoted macrophage  
 recruitment and mediated the development of vascular  
 dissection through the transcription-3 signaling pathway (19).  
 Ye *et al.* found that CD4 T cell infiltration was closely related  
 to aortic root inflammation and the degree of root dilation in  
 TAA patients (20).

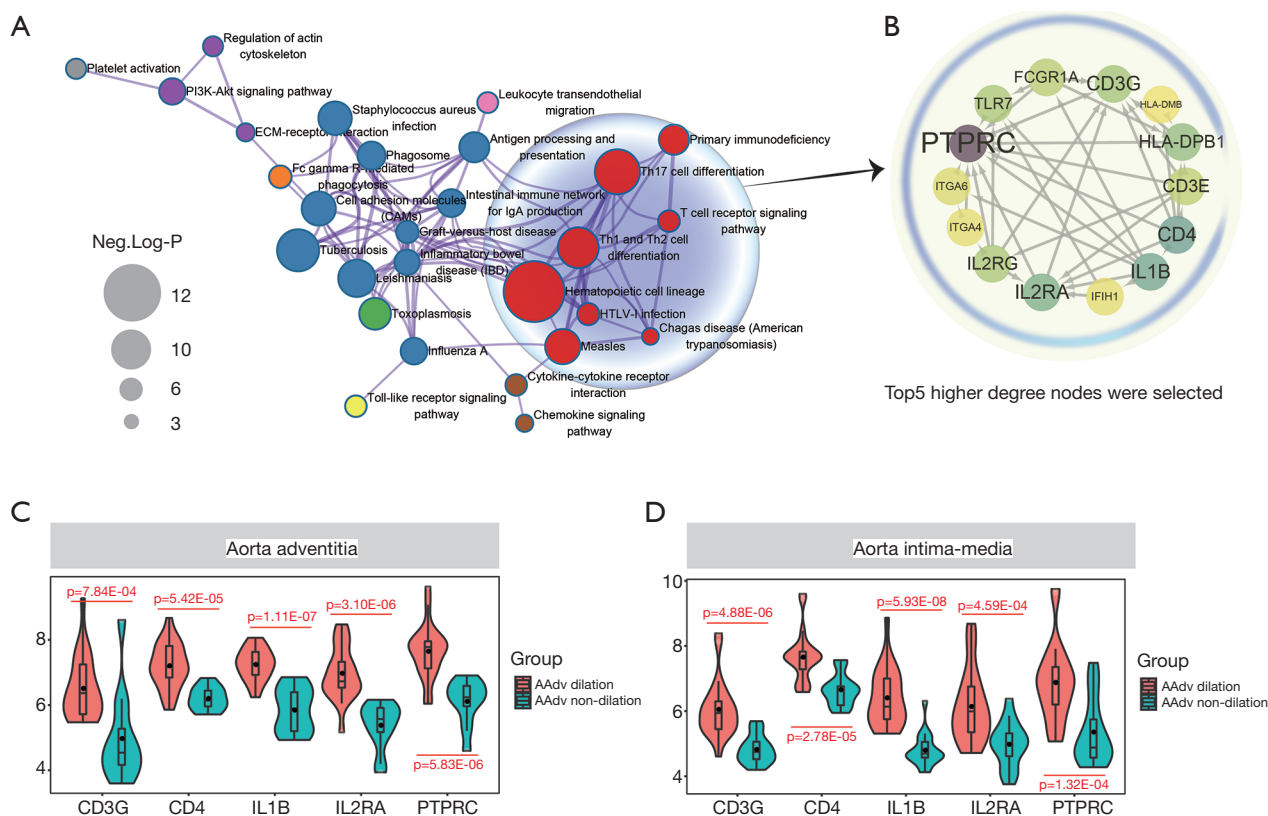


**Figure 3** The construction of the protein-protein interaction (PPI) and KEGG pathway network. *Figure 3A* represents the KEGG pathway network. The dot size represents the negative Log(P value). After extracting the hub genes of the significant pathway, the PPI network was constructed via the STRING database for interesting modules with a threshold value  $>0.4$  in *Figure 3B*. The size of the font represents the degree of gene interaction. *Figure 3C,D* shows the expression analysis of the candidate genes.

311 The comparison between dilated and nondilated vascular  
 312 walls revealed that resting memory CD4<sup>+</sup> T cells were  
 313 significantly infiltrated in the dilated AAdv and AMed tissues,  
 314 especially the AAdv tissues. Crotty believes that memory  
 315 CD4 T cells have a degree of plasticity and can differentiate  
 316 into other subtypes of T cells; however, no experimental  
 317 data have confirmed the plasticity or differentiation ability of  
 318 resting memory CD4 T cells (21). McKinstry *et al.* suggested  
 319 that memory CD4 T cells can not only differentiate into  
 320 subcells such as secretory T cells (Th) but also secrete a large  
 321 amount of cytokines to recruit immune cells and enhance the  
 322 immune response, facilitating the immune response of CD8<sup>-</sup>  
 323 T cells and B cells (22). Sbrana *et al.* found that the degree  
 324 of CD4<sup>+</sup> T lymphocyte infiltration was increased and the  
 325 production of IFN- $\gamma$ , IL-17a, and IL-21 was increased in the  
 326 vascular tissues of patients with ascending aortic dilation (23).  
 327 Jones *et al.* found that compared with other immune cells,  
 328 effector memory and central memory CD4<sup>+</sup> T cells showed

329 higher levels of glycolysis and oxidative phosphorylation and  
 330 a higher metabolic capacity, and regulation of this metabolic  
 331 capacity and cell recruitment were closely related to early  
 332 activation of naïve CD4<sup>+</sup> T cells (24).

333 In addition, our study suggested that IL1B, CD3G,  
 334 CD4, IL2RA, and PTPRC may be the core regulatory  
 335 genes of disease progression in TAV-associated TAAs and  
 336 that these genes are positively correlated with the degree of  
 337 infiltration of resting memory CD4 T cells. Cochain *et al.*  
 338 performed single-cell sequencing on mouse aortic arch  
 339 CD45<sup>+</sup> macrophages in a low-fat diet group and a high-fat  
 340 diet group and found that IL1B was closely associated with  
 341 the inflammatory status of aortic arch endothelial cells (25).  
 342 Yang *et al.* found that miR-30c could participate in the  
 343 process of vascular dilation of abdominal aortic aneurysms  
 344 (AAAs) by targeting IL1B, phosphatidylinositol-4,5-  
 345 bisphosphate 3-kinase catalytic subunit delta (PIK3CD),  
 346 and Ras-related C3 botulinum toxin substrate 2 (RAC2) (26).

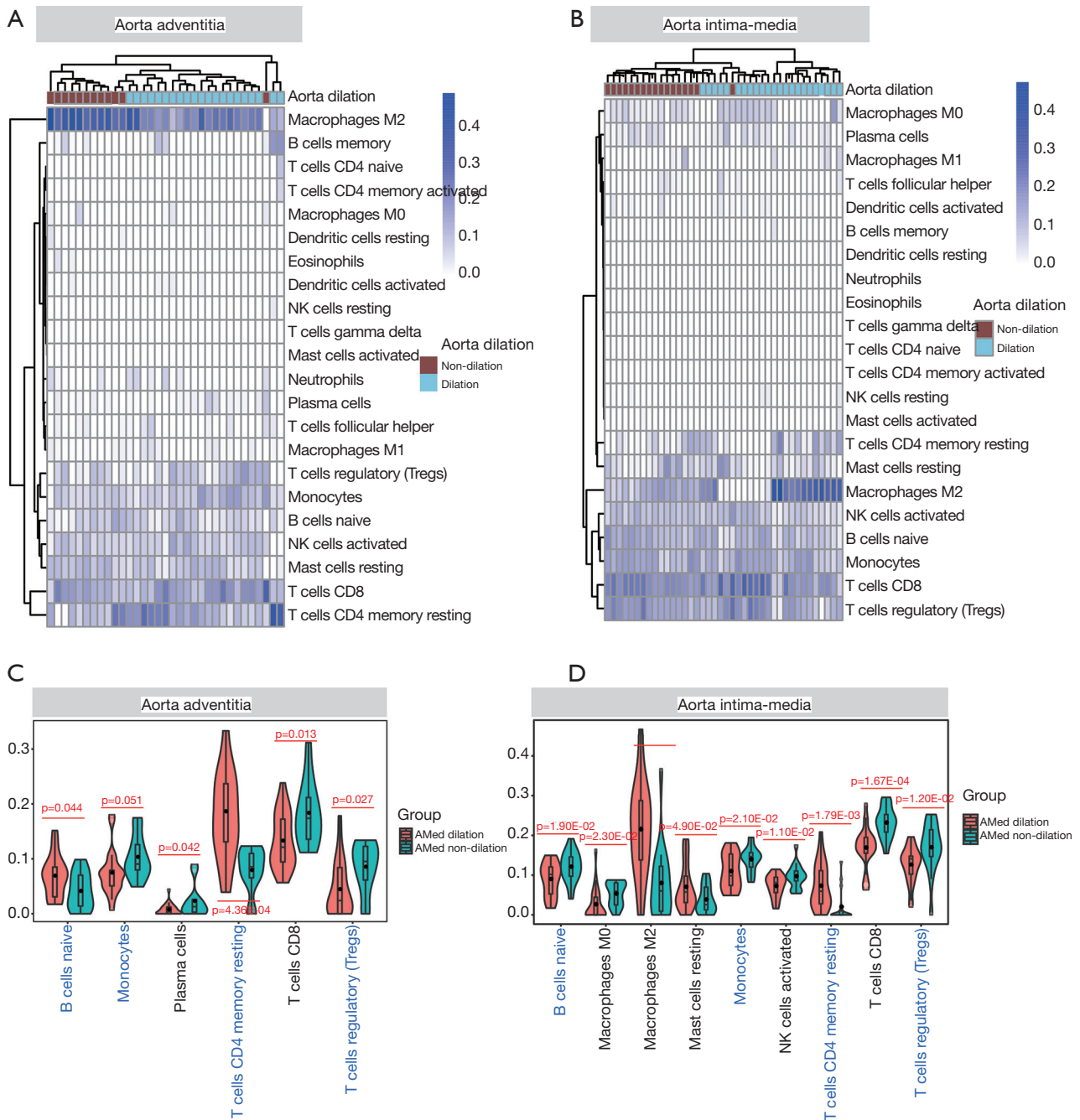


**Figure 4** Detection of immunocyte infiltration and the significant immunocyte subtypes. The hierarchical clustering map of *Figure 4A,B* shows the immunocyte infiltration difference between dilated and nondilated AMed or AAdv samples, respectively. The boxplots of *Figure 4C,D* presenting the significantly infiltrated immunocyte subtypes involved in AMed or AAdv dilation.

347 CD3G is an important regulatory factor during the process  
 348 of T cell development and differentiation (27) and is highly  
 349 expressed in the torn vascular tissues of patients with acute  
 350 aortic dissection (D13). Goudy *et al.* showed that IL2RA

mutations can significantly affect the function of regulatory 351  
 and effector T cells, which are associated with lymphocyte 352  
 proliferation and T cell activation and are the key mediators 353  
 of immune function and homeostasis in the body (28). 354



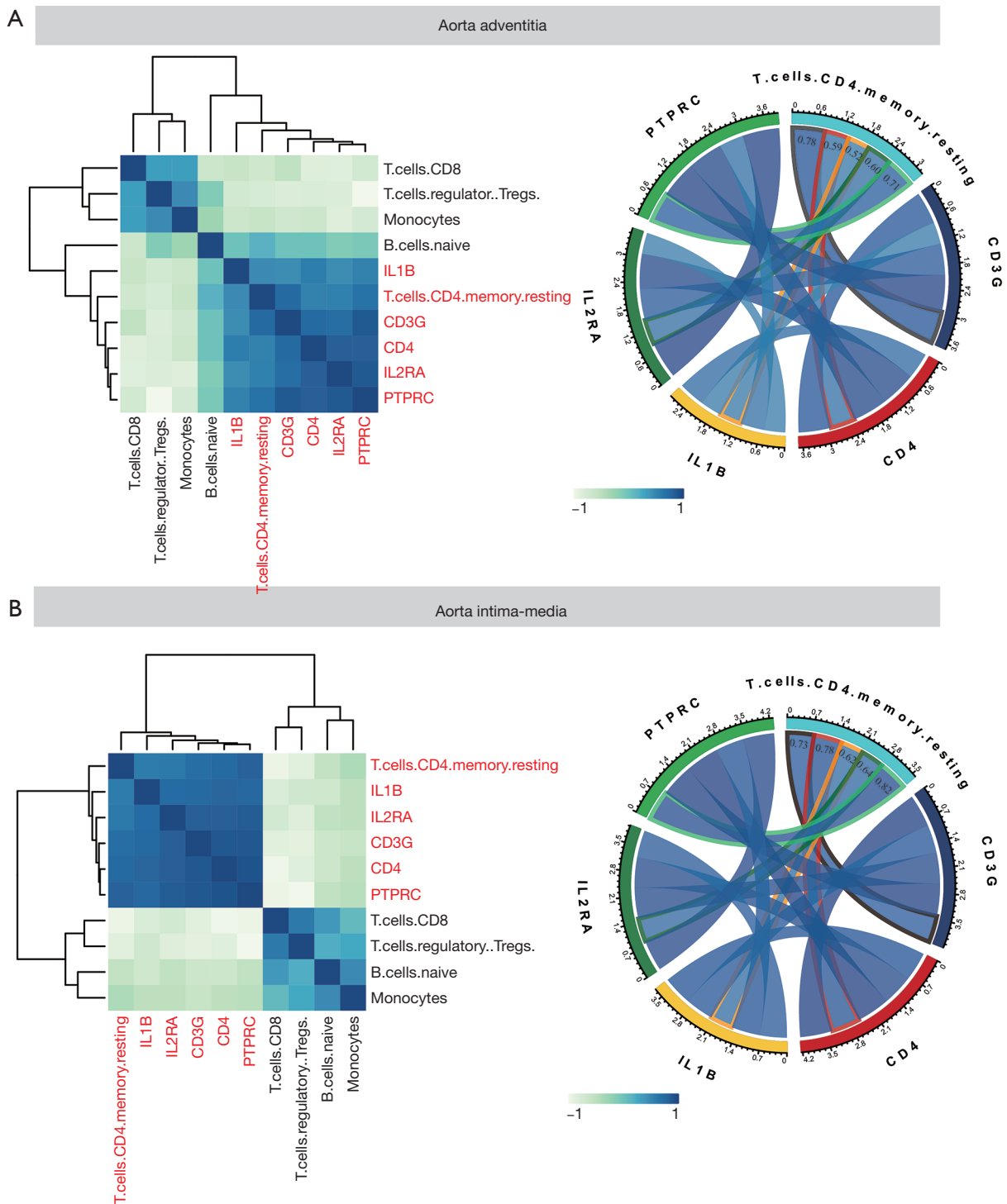


**Figure 5** Interaction analysis of candidate genes and significantly infiltrated immunocyte subtypes. *Figure 5A,B* shows the relationship between immunocytes and hub genes was presented by a clustering heatmap and circus plot with regard to AMed or AAdv dilatation, respectively.

355 Similarly, a study by Belot *et al.* also found that methylation  
 356 of the IL2RA promoter region can affect IL2RA expression  
 357 and T cell activation (29). PTPRC (CD45) is an important  
 358 marker of macrophage and leukocyte activation. Gallo *et al.*  
 359 found that high CD45 expression in TAA patients was  
 360 positively correlated with increased monocyte infiltration  
 361 in the vascular walls and increased IFN- $\gamma$ , IFN-inducible  
 362 protein 10, and IFN-induced T cell  $\alpha$  chemokine levels in  
 363 the circulation (30).

364

365

## Conclusions

366

367

368 In summary, our study found that during the process of  
 369 AAdv and AMed vascular dilation in TAV-associated TAAs,  
 370 PPTRC, IL1B, CD4, CD3G, and IL2RA were involved  
 371 in the regulation of resting memory CD4 T cell tissue  
 372 infiltration, which was closely related to the process of  
 373 vascular dilation. Most of those candidate regulators were  
 374 verified in previous studies. However, several limitations  
 375 remain. First, although the correlations among these  
 376 candidate markers and immunocyte infiltration in TAV-  
 377 associated TAAs were identified, further experimental  
 378 evidence concerning the mechanism is still needed.  
 379 Second, the mechanism of TAV-associated vascular dilation  
 380 is complicated; thus, immunocyte infiltration may be  
 381 important but not essential.

381

382

## Acknowledgments

383

384

385 *Funding:* This work was supported by the Natural Science  
 386 Foundation of Guangdong Province, China (grant  
 387 number 2016A030313792), the Medical Science Research  
 388 Foundation of Guangdong Province, China (grant number  
 389 2016115114137325), the Chinese Medicine Research  
 390 Foundation of Guangdong Province, China (grant number  
 391 20161003), and the National Natural Science Foundation  
 392 of China (NSFC) (grant numbers 81372114 and 81900285).

392

393

## Footnote

394

395

396 *Conflicts of interest:* The authors have no conflicts of interest  
 397 to declare.

397

398 *Ethical Statement:* The authors are accountable for all  
 399 aspects of the work in ensuring that questions related  
 400 to the accuracy or integrity of any part of the work  
 401 are appropriately investigated and resolved. All of the  
 402 microarray data were obtained from the GEO ([https://](https://www.ncbi.nlm.nih.gov/geo/)

[www.ncbi.nlm.nih.gov/geo/](https://www.ncbi.nlm.nih.gov/geo/)) database, and a research ethics  
 application was not needed for this study.

*Open Access Statement:* This is an Open Access article  
 distributed in accordance with the Creative Commons  
 Attribution-NonCommercial-NoDerivs 4.0 International  
 License (CC BY-NC-ND 4.0), which permits the non-  
 commercial replication and distribution of the article with  
 the strict proviso that no changes or edits are made and the  
 original work is properly cited (including links to both the  
 formal publication through the relevant DOI and the license).  
 See: <https://creativecommons.org/licenses/by-nc-nd/4.0/>.

## References

1. McClure RS, Brogly SB, Lajkosz K, et al. Epidemiology and management of thoracic aortic dissections and thoracic aortic aneurysms in Ontario, Canada: A population-based study. *J Thorac Cardiovasc Surg* 2018;155:2254-64.e4.
2. Olsson C, Thelin S, Stahle E, et al. Thoracic aortic aneurysm and dissection: increasing prevalence and improved outcomes reported in a nationwide population-based study of more than 14,000 cases from 1987 to 2002. *Circulation* 2006;114:2611-8.
3. Olsson C, Eriksson N, Stahle E, et al. Surgical and long-term mortality in 2634 consecutive patients operated on the proximal thoracic aorta. *Eur J Cardiothorac Surg* 2007;31:963-9; discussion 969.
4. Sun X, Zhang H, Zhu K, et al. Patient-specific three-dimensional printing for Kommerell's diverticulum. *Int J Cardiol* 2018;255:184-7.
5. Kim JH, Na CY, Choi SY, et al. Integration of gene-expression profiles and pathway analysis in ascending thoracic aortic aneurysms. *Ann Vasc Surg* 2010;24:538-49.
6. Tang PC, Yakimov AO, Teesdale MA, et al. Transmural inflammation by interferon-gamma-producing T cells correlates with outward vascular remodeling and intimal expansion of ascending thoracic aortic aneurysms. *Faseb j* 2005;19:1528-30.
7. Sprague AH, Khalil RA. Inflammatory cytokines in vascular dysfunction and vascular disease. *Biochem Pharmacol* 2009;78:539-52.
8. Folkersen L, Wagsater D, Paloschi V, et al. Unraveling divergent gene expression profiles in bicuspid and tricuspid aortic valve patients with thoracic aortic dilatation: the ASAP study. *Mol Med* 2011;17:1365-73.
9. Barrett T, Wilhite SE, Ledoux P, et al. NCBI GEO: archive for functional genomics data sets--update. *Nucleic*

- 451 Acids Res 2013;41:D991-5.
- 452 10. Ritchie ME, Phipson B, Wu D, et al. limma powers  
453 differential expression analyses for RNA-sequencing and  
454 microarray studies. *Nucleic Acids Res* 2015;43:e47.
- 455 11. Yu G, Wang LG, Han Y, et al. clusterProfiler: an R  
456 package for comparing biological themes among gene  
457 clusters. *Omics* 2012;16:284-7.
- 458 12. Zhou Y, Zhou B, Pache L, et al. Metascape provides a  
459 biologist-oriented resource for the analysis of systems-  
460 level datasets. *Nat Commun* 2019;10:1523.
- 461 13. Chen B, Khodadoust MS, Liu CL, et al. Profiling Tumor  
462 Infiltrating Immune Cells with CIBERSORT. *Methods*  
463 *Mol Biol* 2018;1711:243-59.
- 464 14. Szklarczyk D, Morris JH, Cook H, et al. The STRING  
465 database in 2017: quality-controlled protein-protein  
466 association networks, made broadly accessible. *Nucleic*  
467 *Acids Res* 2017;45:D362-8.
- 468 15. Shannon P, Markiel A, Ozier O, et al. Cytoscape:  
469 a software environment for integrated models of  
470 biomolecular interaction networks. *Genome Res*  
471 2003;13:2498-504.
- 472 16. Pisano C, Balistreri CR, Ricasoli A, et al. Cardiovascular  
473 Disease in Ageing: An Overview on Thoracic Aortic  
474 Aneurysm as an Emerging Inflammatory Disease.  
475 *Mediators Inflamm* 2017;2017:1274034.
- 476 17. Balistreri CR, Buffa S, Allegra A, et al. A Typical Immune  
477 T/B Subset Profile Characterizes Bicuspid Aortic Valve: In  
478 an Old Status? *Oxid Med Cell Longev* 2018;2018:5879281.
- 479 18. Itani HA, McMaster WG, Jr., Saleh MA, et al. Activation  
480 of Human T Cells in Hypertension: Studies of Humanized  
481 Mice and Hypertensive Humans. *Hypertension*  
482 2016;68:123-32.
- 483 19. Ju X, Ijaz T, Sun H, et al. Interleukin-6-signal transducer  
484 and activator of transcription-3 signaling mediates aortic  
485 dissections induced by angiotensin II via the T-helper  
lymphocyte 17-interleukin 17 axis in C57BL/6 mice.  
*Arterioscler Thromb Vasc Biol* 2013;33:1612-21.
20. Ye P, Chen W, Wu J, et al. GM-CSF contributes to aortic  
aneurysms resulting from SMAD3 deficiency. *J Clin Invest*  
2013;123:2317-31.
21. Crotty S. Do Memory CD4 T Cells Keep Their Cell-  
Type Programming: Plasticity versus Fate Commitment?  
Complexities of Interpretation due to the Heterogeneity  
of Memory CD4 T Cells, Including T Follicular Helper  
Cells. *Cold Spring Harb Perspect Biol* 2018. doi: 10.1101/  
cshperspect.a032102.
22. McKinstry KK, Strutt TM, Swain SL. The potential of  
CD4 T-cell memory. *Immunology* 2010;130:1-9.
23. Sbrana S, Tiwari KK, Bevilacqua S, et al. Relationships  
Between Phenotype and Function of Blood CD4+  
T-Cells and Ascending Thoracic Aortic Aneurysm: an  
Experimental Study. *Braz J Cardiovasc Surg* 2019;34:8-16.
24. Jones N, Vincent EE, Cronin JG, et al. Akt and STAT5  
mediate naive human CD4+ T-cell early metabolic  
response to TCR stimulation. *Nat Commun* 2019;10:2042.
25. Cochain C, Vafadarnejad E, Arampatzi P, et al. Single-  
Cell RNA-Seq Reveals the Transcriptional Landscape  
and Heterogeneity of Aortic Macrophages in Murine  
Atherosclerosis. *Circ Res* 2018;122:1661-74.
26. Yang P, Cai Z, Wu K, et al. Identification of key  
microRNAs and genes associated with abdominal aortic  
aneurysm based on the gene expression profile. *Exp*  
*Physiol* 2020;105:160-73.
27. Flanagan BF, Wotton D, Tuck-Wah S, et al. DNase  
hypersensitivity and methylation of the human CD3G  
and D genes during T-cell development. *Immunogenetics*  
1990;31:13-20.
28. Goudy K, Aydin D, Barzaghi F, et al. Human IL2RA  
null mutation mediates immunodeficiency with  
lymphoproliferation and autoimmunity. *Clin Immunol*  
2013;146:248-61.
29. Belot MP, Castell AL, Le Fur S, et al. Dynamic  
demethylation of the IL2RA promoter during in vitro  
CD4+ T cell activation in association with IL2RA  
expression. *Epigenetics* 2018;13:459-72.
30. Gallo A, Saad A, Ali R, et al. Circulating interferon-  
gamma-inducible Cys-X-Cys chemokine receptor 3  
ligands are elevated in humans with aortic aneurysms  
and Cys-X-Cys chemokine receptor 3 is necessary for  
aneurysm formation in mice. *J Thorac Cardiovasc Surg*  
2012;143:704-10.

Cite this article as: Fan X, Peng J, Lei L, He J, Huang J, Zheng D, Xu W, Cai S, Chen J. Integrated analysis of immunocyte infiltration and differential gene expression in tricuspid aortic valve-associated thoracic aortic aneurysms. *Ann Transl Med* 2020;8(6):285. doi: 10.21037/atm.2020.03.05